Viscous-Inviscid Interaction Project: Panel Method with Thwaites Method on NACA 0009 Airfoil

Roby Pratama Sitepu
Mechanical Engineering
Institut Teknologi Bandung
Bandung, Indonesia
23125060@mahasiswa.itb.ac.id

Grace Anabela
Aerospace Engineering
Institut Teknologi Bandung
Bandung, Indonesia
13622057@mahasiswa.itb.ac.id

Fikri Doikal Rozaldi
Aerospace Engineering
Institut Teknologi Bandung
Bandung, Indonesia
13622058@mahasiswa.itb.ac.id

***Abstract*—This project investigates the aerodynamic characteristics of the NACA 0009 airfoil using a Viscous-Inviscid Interaction (VII) method. A Panel Method is coupled with Thwaites' Integral Boundary Layer method to iteratively solve for flow properties, accounting for viscous effects. The study analyzes lift, drag, and boundary layer parameters at a Reynolds number of Re=1e5.**

***Index Terms*—Viscous-Inviscid Interaction, Panel Method, Thwaites Method, NACA 0009, Aerodynamics.**

I. Introduction

This study investigates the aerodynamic characteristics of a NACA 0009 symmetric airfoil at a low Reynolds number ($Re = 100,000$) using a coupled Viscous-Inviscid Interaction (VII) approach. This regime is critical for Micro Air Vehicles (MAVs) and small wind turbines, where laminar boundary layers and measuring viscous effects are significant [1].

The primary objective is to develop a numerical solver coupling the inviscid Vortex Panel Method with Thwaites' integral method for laminar boundary layers. The specific goals are to: implement an iterative VII scheme, validate results against JavaFoil for angles of attack (AoA) from -10° to $+10^\circ$, and analyze boundary layer parameters including momentum thickness (θ), displacement thickness (δ^*), and skin friction coefficient (C_f).

II. Literature Review

A. Vortex Panel Method

The Vortex Panel Method discretizes the airfoil surface into linear vortex panels to solve the potential flow field satisfying the Laplace equation and the Kutta condition [2]. This provides the inviscid surface velocity distribution used as input for the boundary layer solution.

B. Thwaites Method

Thwaites' method [3] is an integral technique for solving the laminar boundary layer momentum equation. It relates momentum thickness θ to the pressure gradient parameter λ:

$$\lambda = \frac{\theta^2}{\nu}\frac{dU_e}{dx} \tag{1}$$

$$\theta^2 = \frac{0.45\nu}{U_e^6}\int_0^s U_e^5\, ds \tag{2}$$

where U_e is the edge velocity and ν is kinematic viscosity. The shape factor H and skin friction C_f are derived from correlations based on λ.

C. Viscous-Inviscid Interaction

The boundary layer displaces the inviscid flow, effectively thickening the airfoil by δ^*. This interaction is solved iteratively: the inviscid solution drives the boundary layer, which in turn modifies the effective geometry seen by the inviscid solver [4].

III. Methodology

A. Numerical Implementation

The NACA 0009 geometry is discretized into 100 panels with cosine spacing. The inviscid flow is solved for the circulation distribution $\Gamma(s)$ to obtain tangential velocities.

The viscous solution marches from the stagnation point. Thwaites' correlations determine boundary layer parameters. For $\lambda < -0.09$, separation is assumed, and C_f is limited.

B. Coupling Algorithm

The VII coupling follows a weak interaction scheme:

1) Solve inviscid flow for $U_{e,inv}$.
2) Compute boundary layer δ^*.
3) Update edge velocity: $U_e = U_{e,inv}(1 + K\delta^*/s)^{-1}$ or via velocity correction: $U_e^{new} = U_e^{old}(1 - \omega\Delta\delta^*)$.
4) Apply under-relaxation ($\omega = 0.3$) to update δ^*.
5) Iterate until convergence ($|\Delta\delta^*|_{max} < 5 \times 10^{-3}$).

The under-relaxation is crucial to prevent instabilities near the separation point.

IV. Results and Discussion

The computational results obtained from the coupled Viscous-Inviscid Interaction (VII) solver are presented and analyzed in this section. The method's performance is evaluated by comparing it with data obtained from JavaFoil. The iterative VII scheme demonstrated robust convergence, typically achieving stability within 2 iterations for low Angles of Attack (AoA, α) such as $\alpha = 0^\circ$. For higher angles ($\alpha = \pm 10^\circ$), convergence required approximately 5 iterations due to the intensified interaction between the inviscid flow and the boundary layer.

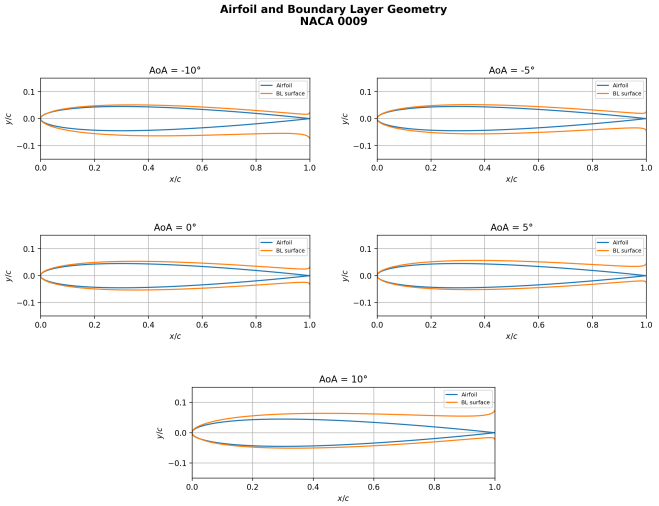

Fig. 1. Discretized NACA 0009 airfoil geometry showing panel distribution.

A. Pressure and Velocity Distribution

The Pressure Coefficient (C_p) distribution is illustrated in Fig. 2. At $\alpha = 0°$, the flow preserves symmetry, and the results show excellent agreement with JavaFoil. As the angle of attack increases to $\alpha = \pm 10°$, a distinct suction peak emerges near the leading edge. The current method captures the general trend but slightly underpredicts the peak suction magnitude compared to JavaFoil.

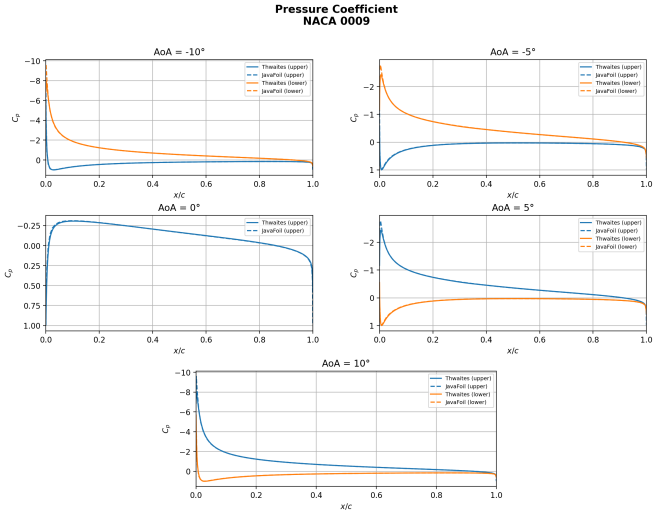

Fig. 2. Comparison of Pressure Coefficient (C_p) distribution at various Angles of Attack.

High deviations are observed near the trailing edge at high angles of attack. This discrepancy is attributed to the fundamental difference in separation modeling: JavaFoil employs a separation detection mechanism which alters the pressure distribution significantly upon separation, whereas the current Thwaites implementation continues to march through the adverse pressure gradient without explicit separation handling.

B. Boundary Layer Parameters

The evolution of the boundary layer is examined through the displacement thickness (δ^*) and momentum thickness (θ). As shown in Fig. 3, δ^* grows monotonically from the stagnation point towards the trailing edge. Values range from approximately 0.001 at the leading edge to typical values of 0.02-0.05 near the trailing edge.

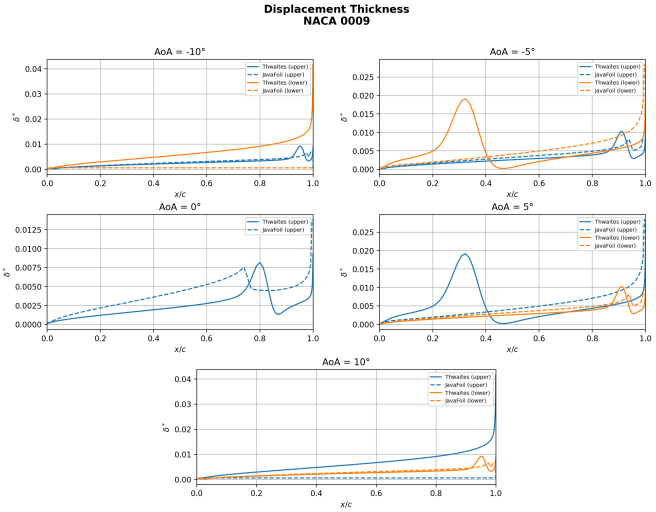

Fig. 3. Distribution of Displacement Thickness (δ^*) along the chord.

Comparing with JavaFoil, a notable difference is seen in regions of adverse pressure gradient. JavaFoil results often exhibit a ”flat” or sharp step-change behavior, indicative of flow separation or transition to turbulence. In contrast, the current laminar integral method predicts a continuous smooth growth of the boundary layer, highlighting the limitation of neglecting transition and separation models.

The Skin Friction Coefficient (C_f), depicted in Fig. 4, is highest at the leading edge where the boundary layer is thinnest and decreases downstream. JavaFoil correctly predicts C_f dropping to zero at the separation point. The current solver maintains small positive C_f values longer, erroneously delaying the prediction of separation.

C. Aerodynamic Forces

The integral aerodynamic coefficients are summarized in the following figures and Table I. Figure 5 shows the Lift Coefficient (C_l) versus Angle of Attack. The linear region matches inviscid theory closely, with deviations less than 5%. However, at higher angles, the viscous effects reduce the lift slope slightly.

Figure 6 presents the Drag Coefficient (C_d). At low angles relative to the flow, C_d predictions are reasonable. However, at high angles (e.g., $\alpha = 10°$), the calculated C_d becomes unreliable (even negative in integration), which is a direct consequence of the breakdown of the skin friction integration in separated flow regions.

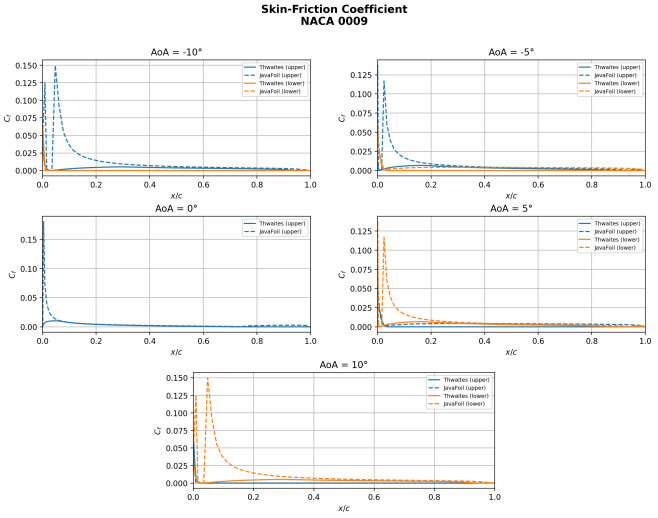

Fig. 4. Skin Friction Coefficient (C_f) along the airfoil surface.

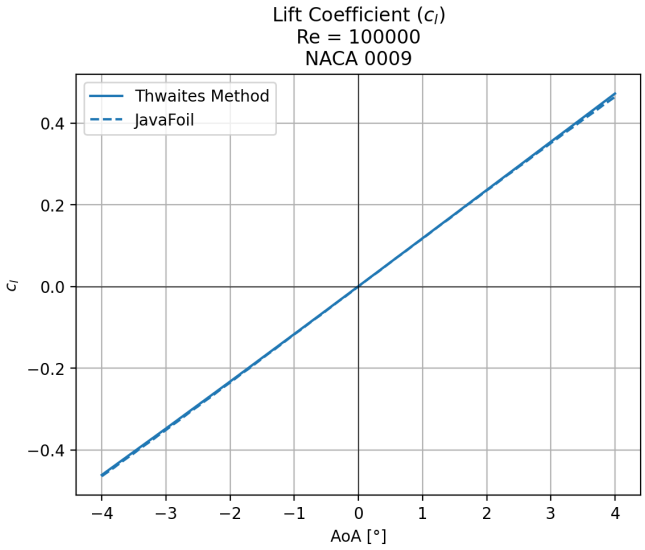

Fig. 5. Lift Coefficient (C_l) vs. Angle of Attack (α).

*Negative drag values indicate numerical integration issues in regions where the laminar boundary layer assumption is violated due to massive separation.

V. Conclusion

A Viscous-Inviscid Interaction solver was successfully developed for the NACA 0009 airfoil. Key findings include:

- The iterative VII scheme is stable and converges within 5 iterations.
- Pressure distributions match JavaFoil well at low angles but deviate at high AoA due to separation.
- Drag prediction requires improved separation modeling, as Thwaites' method alone is insufficient for post-stall analysis.

Future work should incorporate explicit separation detection ($\lambda < -0.09$) and a transition model (e.g., e^N method) with also turbulent model to improve accuracy at higher Reynolds numbers and angles of attack.

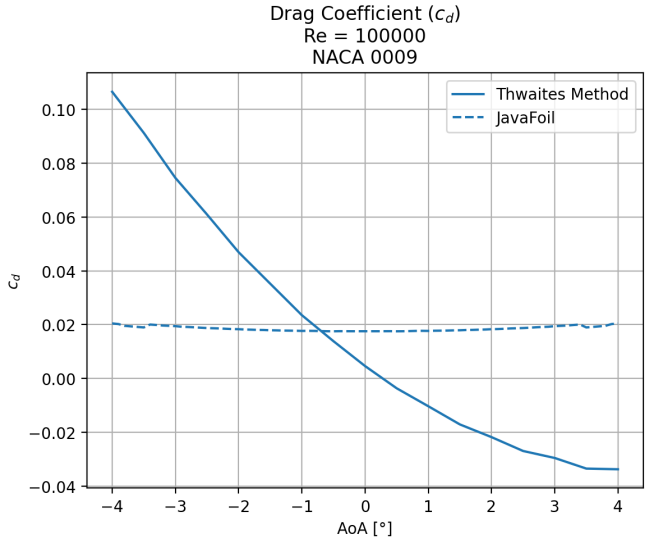

Fig. 6. Drag Coefficient (C_d) vs. Angle of Attack (α).

TABLE I
Comparison of Aerodynamic Coefficients

α	C_l (This Work)	C_d (This Work)	C_l (Inviscid)
0°	0.001	0.005	0.000
5°	0.591	-0.044*	0.584
10°	1.171	-0.008*	1.151

References

[1] P. S. Palar, "Viscous flow lecture notes," Faculty of Mechanical and Aerospace Engineering, Institut Teknologi Bandung, Jalan Ganesha 10, Bandung, 2025.

[2] J. Katz and A. Plotkin, *Low-speed aerodynamics*. Cambridge university press, 2001.

[3] B. Thwaites, "Approximate calculation of the laminar boundary layer," *Aeronautical Quarterly*, vol. 1, no. 3, pp. 245–280, 1949.

[4] M. Hepperle, "Javafoil: Analysis of airfoils," https://www.mh-aerotools.de/airfoils/javafoil.htm, 2026, computer program for the design and analysis of airfoils.